WATER RESOURCES RESEARCH, VOL. 38, NO. 4, 1035, 10.1029/2000WR000022, 2002

Conditional first-order second-moment method and its application to the quantification of uncertainty in groundwater modeling

Harald Kunstmann

Institute for Meteorology and Climate Research-Atmospheric Environmental Research, Karlsruhe Research Center Technology and Environment, Garmisch-Partenkirchen, Germany

Wolfgang Kinzelbach and Tobias Siegfried

Institute for Hydromechanics and Water Resources Management, Swiss Federal Institute of Technology Zürich, Zürich, Switzerland

Received 16 October 2000; revised 4 June 2001; accepted 4 September 2001; published 10 April 2002.

[1] Decision making in water resources management usually requires the quantification of uncertainties. Monte Carlo techniques are suited for this analysis but imply a huge computational effort. An alternative and computationally efficient approach is the first-order second-moment (FOSM) method which directly propagates parameter uncertainty into the result. We apply the FOSM method to both the groundwater flow and solute transport equations. It is shown how conditioning on the basis of measured heads and/or concentrations yields the ''principle of interdependent uncertainty'' that correlates the uncertainties of feasible hydraulic conductivities and recharge rates. The method is used to compute the uncertainty of steady state heads and of steady state solute concentrations. It is illustrated by an application to the Palla Road Aquifer in semiarid Botswana, for which the quantification of the uncertainty range of groundwater recharge is of prime interest. The uncertainty bounds obtained by the FOSM method correspond well with the results obtained by the Monte Carlo method. The FOSM method, however, is much more advantageous with respect to computational efficiency. It is shown that at the planned abstraction rate the probability of exceeding the natural replenishment of the Palla Road Aquifer by overpumping is 30%. *INDEX TERMS:* 1832 Hydrology: Groundwater transport; 1869 Hydrology: Stochastic processes; 3260 Mathematical Geophysics: Inverse theory; 9305 Information Related to Geographic Region: Africa; *KEYWORDS:* uncertainty propagation, inverse stochastic modeling, groundwater recharge, first-order second-moment method, Monte Carlo method, environmental tracer

1. Introduction

[2] Groundwater models are widely used although their predictive power is limited because of the uncertainty of the model parameters. The reliability of predictions depends on the accuracy of available knowledge of aquifer structure, boundary conditions, aquifer parameters, and future hydrological input parameters as well as on errors, because models are, in general, simplified versions of reality. Lacking aquifer parameters can be estimated by fitting modeled piezometric heads (and/or concentrations) to measurements made in the past. However, even a perfectly calibrated model cannot entirely remove uncertainty because the inverse problem does not necessarily have a unique solution.

[3] Imperfect knowledge of aquifer parameters can be expressed by giving sets or distributions of input parameters instead of single values, e.g., a set of transmissivities and/or recharge rates. If the resulting range of the possible drawdowns or concentrations at an observation point is known, the probability of failure of a proposed management or remediation scheme can be estimated, and conservative scenarios can be designed.

[4] The Monte Carlo Method is widely used in stochastic modeling. It is a versatile method which, in principle, can always be applied. It consists of performing a large number of deterministic calculations for random realizations of the problem and a statistical analysis of results. The computational effort may become huge, however, before results converge, and the number of realizations necessary is at best only approximately known in advance.

[5] An alternative and computationally efficient approach is the first-order second-moment technique (FOSM) [*Dettinger and Wilson*, 1981] which directly propagates the uncertainty originating from parameter uncertainty. It can be applied in all cases where the parameter variances are moderate.

[6] The basic idea for the first-order second-moment (FOSM) method applied to groundwater problems was introduced by *Dettinger and Wilson* [1981]. *Townley and Wilson* [1985] generalized this approach to include unsteady flows and the effect of randomness in the storage coefficient and in the boundary conditions. Whereas *Dettinger* [1979] concentrated on a one-dimensional example, *Townley* [1983] verified the FOSM method for a problem in two dimensions by comparing the results with the Monte Carlo results presented by *Smith and Freeze* [1979]. The original formulation of the FOSM method [*Dettinger and Wilson*, 1981; *Townley and Wilson*, 1985] includes a computationally efficient way of calculating sensitivity matrices that does not require the repeated evaluation of the system equation. This technique for calculating the sensitivity matrices has been applied to the groundwater flow equation but not yet to the transport equation. Applications so far have been for simple configurations with a small number of nodes. Conditioning of the uncertainty propagation by head or concentration measurements within the FOSM method, as it is presented in this work, was not performed.

[7] A modified approach of the FOSM method, which computes sensitivity matrices by the repeated evaluation of the system

0043-1397/02/2000WR000022$09.00

equation, was applied to a few field studies. *James and Oldenburg* [1997] used the FOSM method to describe a trichlorethylene contamination. *Tiedemann and Gorelick* [1993] applied it to the optimization of a groundwater contaminant capture design.

[8] Besides the FOSM method another numerical approach has been used to treat stochastic groundwater flow: The distributed parameter approach (DPA) is based on the differential equations describing the mean and covariance of head. This approach has been developed in detail by *McLaughlin and Wood* [1988] and was explored in earlier work by *Tang and Pinder* [1977] and *Devary and Doctor* [1982]. *Graham and McLaughlin* [1989a, 1989b] used the DPA to derive expressions for predicting uncertainty in a solute transport exercise and compared the results to Monte Carlo analysis. The FOSM and the DPA are based on different Taylor series approximations; however, the expansion is made around the same set of variables. With FOSM the piezometric head (or solute concentration matrix) is expanded around the model parameters and substituted into the definition for the head (or solute concentration) covariance matrix, whereas DPA is based on approximating matrix terms in a spatially discretized model system of equations, perturbed around the model parameters. The second difference is the manner in which the temporal discretization is made. For DPA the temporal discretization is made on the head covariance equation, whereas with FOSM a temporally discretized Taylor series of the head equation is substituted into the head covariance [*Kunstmann*, 1998]. At steady state the two methods DPA and FOSM yield the same expression for the head covariance matrix. The transient expressions for the head covariance matrices differ, while the transient expressions for the cross-covariance matrices (between heads and parameters) are found to be identical [*Connell*, 1995; *Kunstmann*, 1998]. Another important difference between the DPA and the FOSM approach, as presented in this work, is that the FOSM method calculates the uncertainty propagation for the coupled flow and transport equation. First, the covariance matrix of the piezometric heads and the mixed parameter head covariance matrices are calculated by the uncertainty propagation based on the flow equation. These three covariance matrices, in turn, are prerequisites for the calculation of the covariance matrix of the solute concentration. The requirements of smallness of parameter variability are the same for both methods as they are both linear. Other early papers [e.g., *Delhomme*, 1979; *Clifton and Neumann*, 1982; *Cooley*, 1979] have addressed the estimation of the covariance of predicted heads due to uncertain parameters using other techniques. The application of derived head statistics to Bayesian estimation is discussed, for example, by *Hoeksema and Kitanidis* [1985] and *Dagan* [1982].

[9] If the probability associated with a limited number of "failure" states is of interest, the first-order reliability method (FORM) can be used as a computationally efficient alternative to Monte Carlo simulations. Such questions arise in the context of safety assessments, where the probability of exceeding a target risk level or a corresponding concentration threshold has to be determined. In FORM the exceedance probability is approximated to first order. The FORM method was originally developed in the field of structural reliability [*Ang and Tang*, 1984; *Madsen et al.*, 1986] and has been applied for uncertainty analyses of environmental flow and transport problems since [*Sitar et al.*, 1987; *Hamed et al.*, 1995; *Xiang and Mishra*, 1997; *Skaggs and Barry*, 1997].

[10] In this paper, the FOSM method is presented in a way that is suitable for field case applications. The FOSM is embedded in a finite difference approach and applied to both the partial differential equations of groundwater flow and solute transport. We extend the method to conditional analysis, showing how the introduction of measurements of piezometric heads or solute concentrations influence the uncertainty propagation. Closed formulae obtained by the method clearly explain how conditioning information diminishes the uncertainty of model output. These formulae quantify the uncertainty arising from the nonuniqueness of the inverse problem. This "principle of interdependent uncertainty" shows how the uncertainties of hydraulic conductivity (or transmissivity) and groundwater recharge are related to each other in the presence of head or concentration measurements. The influence of model and measurement errors is included. The proposed method is applied to a case study in semiarid Botswana where the quantification of groundwater recharge and its uncertainty bounds were of prime interest. FOSM results are compared to results from a Monte Carlo calculation.

[11] For a further example of the FOSM method the reader is referred to *Kunstmann and Kinzelbach* [2000], who show the application of the unconditional and conditional FOSM method to the computation of stochastic wellhead protection zones for an aquifer in Gambach (Germany) by combining the FOSM method and Kolmogorov backward equation analysis. In contrast to *Kunstmann and Kinzelbach* [2000] this paper introduces the theory of unconditional and conditional FOSM method in detail as well as the incorporation of model/measurement error.

2. Theory

2.1. The FOSM Method: Unconditional Moments

[12] The numerical solution of the two-dimensional steady state groundwater flow equation for confined aquifers

$$\nabla \cdot \left(mk_f \nabla h\right) + q = 0 \tag{1}$$

is usually obtained by finite element or finite difference schemes for unknown piezometric head h at specified grid points, represented as a vector $\mathbf{h}$. The aquifer parameters, such as the hydraulic conductivity k_f (length time $^{-1}$), the thickness of the aquifer m (length), and the recharge/discharge rates q (length^3 time $^{-1}$ length $^{-2}$) can also be specified as vectors $\mathbf{p}$ at all grid points.

[13] In subsurface hydrology, flow parameters such as hydraulic conductivity are often found to be lognormally distributed in space [*Gelhar*, 1993]. In the following it is assumed that both the hydraulic conductivity k_f and the groundwater recharge q are lognormally distributed. Thus $Y = \ln k_f$ and $Z = \ln q$ are normally distributed stochastic variables. Whereas the assumption of a lognormally distributed hydraulic conductivity is experimentally well justified [e.g., *Gelhar*, 1993], a lognormally distributed groundwater recharge, however, is assumed for purely practical reasons: When applying parameter estimation algorithms, as performed in the application presented in this work, positive values for groundwater recharge are always obtained. The assumption of lognormally distributed k_f and q is not a restriction to the generality of the method. Everything could be also derived for quantities q and k_f instead of Y and Z. The aquifer parameters $\mathbf{p}$ (i.e., log hydraulic conductivity Y or log recharge Z) are assumed to be uncertain. They are described under the preceding assumptions as having a mean value $\mathbf{p}$ and a covariance Cov ($\mathbf{p}$). If the model setup is based on a zonation of log hydraulic conductivity, the elements of $\mathbf{Y}$ are given by zonal values of $Y : \mathbf{Y} \in \Re^{N_Y}$, with $\Re$

indicating the space of real numbers and with N_Y equal to the number of zones within which log hydraulic conductivity Y is assumed to be uniform. The same can hold for $\mathbf{Z}$. If the zonal values are uncorrelated, Cov_{YY}, and Cov_{ZZ} are of diagonal shape. The entries of the diagonal elements are the squared standard deviations of the uncertainties of the zonal values.

[14] The first moment of the heads is approximated to first-order accuracy [*Dettinger and Wilson*, 1981] by the mean heads $\mathbf{h}$ obtained as the solution of (1) using the mean values of the aquifer parameters $\mathbf{p}$.

$$E[\mathbf{h}(\mathbf{p})] = \hat{\mathbf{h}} \stackrel{1}{=} \mathbf{h}(\hat{\mathbf{p}}). \tag{2}$$

The propagation of parameter uncertainties into the head uncertainties, given by the covariance matrix $\mathrm{Cov}(\mathbf{h})$, can be approximated by inserting the Taylor series expansion of $\mathbf{h}$ into

$$\mathrm{Cov}_{hh} \equiv \mathrm{Cov}(\mathbf{h}) = E\left[\left(\mathbf{h} - \hat{\mathbf{h}}\right) \cdot \left(\mathbf{h} - \hat{\mathbf{h}}\right)\right], \tag{3}$$

yielding

$$\begin{aligned}\mathrm{Cov}_{hh} \stackrel{1}{=} & D_{hY} \cdot \mathrm{Cov}_{YY} \cdot D_{hY}^T + D_{hZ} \cdot \mathrm{Cov}_{ZZ} \cdot D_{hZ}^T \\ & + D_{hZ} \cdot \mathrm{Cov}_{ZY} \cdot D_{hY}^T + D_{hY} \cdot \mathrm{Cov}_{YZ} \cdot D_{hZ}^T,\end{aligned} \tag{4}$$

where the superscript ^{T} denotes the transpose of the matrix. The parameter head cross-covariance matrices are obtained from

$$\mathrm{Cov}_{hY} \equiv E\left[\left(\mathbf{h} - \hat{\mathbf{h}}\right) \cdot \left(\mathbf{Y} - \hat{\mathbf{Y}}\right)\right] \stackrel{1}{=} D_{hY} \cdot \mathrm{Cov}_{YY} + D_{hZ} \cdot \mathrm{Cov}_{ZY} \tag{5}$$

$$\mathrm{Cov}_{hZ} \equiv E\left[\left(\mathbf{h} - \hat{\mathbf{h}}\right) \cdot \left(\mathbf{Z} - \hat{\mathbf{Z}}\right)\right] \stackrel{1}{=} D_{hZ} \cdot \mathrm{Cov}_{ZZ} + D_{hY} \cdot \mathrm{Cov}_{YZ} \tag{6}$$

[*Dettinger and Wilson*, 1981; *Townley and Wilson*, 1985]. The superscript above the equal sign indicates the order of the approximation. $D_{hY} \equiv (D_{\mathbf{Y}^T}\mathbf{h})|_{\mathbf{Y}=\hat{\mathbf{Y}},\,\mathbf{Z}=\hat{\mathbf{Z}}}$ and $D_{hZ} \equiv (D_{\mathbf{Z}^T}\mathbf{h})|_{\mathbf{Y}=\hat{\mathbf{Y}},\,\mathbf{Z}=\hat{\mathbf{Z}}}$ are first derivatives of $\mathbf{h}$ with respect to the transpose of the parameter vectors ($\mathbf{Y}$, $\mathbf{Z}$), evaluated at their mean values. These derivatives are Jacobian matrices expressing the sensitivity of h_i to variations or uncertainties in Y_j and Z_j. In unconditional analysis it is assumed that Z and Y are uncorrelated and that $\mathrm{Cov}_{YZ} = \mathrm{Cov}_{YZ} =$ null matrix. Since the second moments are calculated in first-order accuracy, the method is named the "first-order second-moment method."

[15] The FOSM method is now applied to the two-dimensional (2-D) steady state solute transport equation [e.g., *Bear*, 1972]

$$n_m\left(\nabla \cdot (\mathbf{v}c) - \nabla \cdot \left[\left(D_{\mathrm{mol}} + D_{\mathrm{disp}}\right) \cdot \nabla c\right]\right) - q c_{\mathrm{in}} = 0, \tag{7}$$

where c is solute concentration (mass length^{-3}), $\mathbf{v}$ is 2-D pore velocity vector (length time^{-1}), n_m is mobile porosity [dimensionless], D_{mol} is molecular diffusion coefficient (length^2 time^{-1}), D_{disp} is dispersion tensor (length^2 time^{-1}) according to [*Scheidegger*, 1961], q is recharge per unit horizontal area (length^3 time^{-1} length^{-2}), c_{in} is pollutant concentration in inflows to aquifer (mass length^{-3}), and m is thickness of aquifer (length).

[16] The velocity $\mathbf{v}$ is given by Darcy's law:

$$\mathbf{v} = -\frac{1}{n_m} k_f \nabla h = -\frac{1}{n_m} e^Y \nabla h. \tag{8}$$

The first-order approximation of the mean concentrations $E(\mathbf{c})$ is the solution of the partial differential equation using the mean values of all aquifer parameters,

$$E[\mathbf{c}(\mathbf{Y}, \mathbf{Z}, \mathbf{h})] = \hat{\mathbf{c}} \stackrel{1}{=} c\left(\hat{\mathbf{Y}}, \hat{\mathbf{Z}}, \hat{\mathbf{h}}\right). \tag{9}$$

The covariance of the concentration in steady state can be derived in analogy to the flow equation and is given by

$$\begin{aligned}\mathrm{Cov}_{cc} \stackrel{1}{=} & D_{ch} \cdot \mathrm{Cov}_{hh} \cdot D_{ch}^T + D_{cY} \cdot \mathrm{Cov}_{YY} \cdot D_{cY}^T + D_{cZ} \cdot \mathrm{Cov}_{ZZ} \cdot D_{cZ}^T \\ & + D_{ch} \cdot \mathrm{Cov}_{hY} \cdot D_{cY}^T + D_{cY} \cdot \mathrm{Cov}_{Yh} \cdot D_{ch}^T \\ & + D_{ch} \cdot \mathrm{Cov}_{hZ} \cdot D_{cZ}^T + D_{cZ} \cdot \mathrm{Cov}_{Zh} \cdot D_{ch}^T \\ & + D_{cY} \cdot \mathrm{Cov}_{YZ} \cdot D_{cZ}^T + D_{cZ} \cdot \mathrm{Cov}_{ZY} \cdot D_{cY}^T.\end{aligned} \tag{10}$$

D_{ch}, D_{cY}, and D_{cZ} indicate the sensitivity matrices of the solute concentration with respect to the piezometric heads, log hydraulic conductivity Y, and log recharge Z. The computation of Cov_{cc} requires evaluation of Cov_{hh}, Cov_{hY}, and Cov_{hZ} from (4), (5), and (6). The uncertainty of the concentrations is then described in terms of variances of $\mathbf{c}$, given by σ_c^2, the diagonal elements of Cov_{cc}.

[17] The computational advantage of the FOSM method depends on how the sensitivity matrices are calculated and how matrix multiplications are organized. Details are given by *Kunstmann* [1998]. Thus the rank of the $n \times n$ covariance matrices, such as Cov_{hh} and Cov_{cc}, is the limiting factor for the computational efficiency of the method. If only the variances of the head simulations are of interest, calculation of the diagonal of Cov_{hh} is sufficient. However, if the uncertainties of the solute concentrations are required, all entries of Cov_{hh} must be evaluated. In the application presented in section 3, only the standard deviations of the concentrations are of interest, and thus only the diagonal elements of Cov_{cc} need to be calculated. If only specific grid points are of interest, one can skip the computation for other grid points thus reducing computational effort.

[18] Uncertainty in the dispersion tensor D_{disp} implicitly is included in the analysis as far as it can be traced back to uncertainty in the velocity field. Uncertainty in the velocity field, in general, arises from uncertainty in hydraulic conductivity, piezometric heads, thickness of the aquifer, and porosity (equation (8)). The uncertainty in conductivity and recharge propagates into uncertainty in heads, which, in turn, propagates into uncertainty in the velocity field. Porosity and the thickness of the aquifer are assumed to be known "perfectly." The same holds for dispersivity, which together with the velocity field, constitutes D_{disp}. In principle, there is no difficulty extending the FOSM approach to additional uncertainties such as uncertainty of porosity, thickness of the aquifer, or dispersivities.

[19] In the unconditional case presented so far, the mixed parameter covariances, Cov_{ZY} and Cov_{YZ}, are assumed to vanish; that is, the uncertainties of log recharge and log hydraulic conductivity are assumed to be uncorrelated. In the presence of head or concentration measurements these uncertainties become related to each other as the measurements express the interaction of both. This relationship leads to the conditional FOSM method.

2.2. FOSM Method: Conditional Moments

[20] Usually, estimates of hydraulic conductivity and recharge are obtained by inverse modeling techniques. In a steady state

calibration process, aquifer parameters are varied until measured and simulated heads at the observation points agree as closely as possible, for example, until

$$\chi^2 = \sum_{i=1}^{N} \frac{\left(h_{\text{modeled},i} - h_{\text{observed},i}\right)^2}{\sigma^2_{h_{\text{observed},i}}} \rightarrow \min \Rightarrow \hat{Y}, \hat{Z}, \tag{11}$$

with $\hat{Y}$ and $\hat{Z}$ being the corresponding optimal parameter estimates. Unfortunately, this calibration can lead to nonunique results [e.g., *Carrera and Neumann*, 1986], as different sets of parameters $\hat{Y}$ and $\hat{Z}$ can yield the same distribution of simulated piezometric heads, especially if both fluxes and hydraulic conductivities are unknown. For example, for negligible well discharge, essentially the same head distribution can be obtained for high recharge and high hydraulic conductivity, as well as for low recharge and low hydraulic conductivity. In general, there is a set of combinations of Y and Z that lead to a practically identical model output at the measurement locations. A decisive question of parameter estimation therefore is which set of recharge rates $Z \in \left\{\hat{Z} \pm \sigma_Z\right\}$ will lead to an identical model output at the measurement locations for a given set of possible hydraulic conductivities $Y \in \left\{\hat{Y} \pm \sigma_Y\right\}$.

[21] A "principle of interdependent uncertainty" can be derived from the equations of the unconditional FOSM method using the idea that, if specific entries of Cov_{hh} or Cov_{cc} are known through measurements, the uncertainty propagation equations yield nontrivial correlations between the parameter covariances Cov_{ZZ} and Cov_{YY}. The measurement of a piezometric head at grid point location k gives knowledge of that head within its uncertainty bounds because of measurement errors. Its uncertainty, σ_{h_k}, is therefore reduced to the measurement error $\sigma_h|_{\text{measurement error}}$. All covariance matrix elements composed of factors, σ_{h_k}, such as Cov_{hh}, Cov_{hY}, and Cov_{hZ}, then read (with ρ indicating the correlation coefficient) as follows:

$$\text{Cov}_{hh}\big|_{k,l} = \rho_{h_k h_l} \sigma_{h_k} \sigma_{h_l} \tag{12}$$

if k or l are measurement locations,

$$\text{Cov}_{hY}\big|_{k,i} = \rho_{h_k Y_i} \sigma_{h_k} \sigma_{Y_i} = 0, \quad \forall \text{i} = 1, \ldots, N_Y \tag{13}$$

if k is the measurement location,

$$\text{Cov}_{hZ}\big|_{k,j} = \rho_{h_k Z_j} \sigma_{h_k} \sigma_{Z_j} = 0, \quad \forall j = 1, \ldots, N_Z \tag{14}$$

if k is measurement location. In the example presented, it is assumed that there is no correlation between measurement errors of heads and parameters Y and Z. Therefore (12) reduces to $\text{Cov}_{hh}\big|_{k,k} = \sigma^2_{h_k}$. Equations (12)–(14) determine the relationship between uncertainties in Y and Z when heads are used for conditioning.

[22] To establish the system of equations that determines the relation between Cov_{YY} and Cov_{ZZ}, the $n \times n$ head covariance matrix Cov_{hh} is projected to a $N_h \times N_h$ "measurement subspace," where N_h is the number of head measurements. The projection matrix P has N_h rows and n columns:

$$P \in \Re^{N_h \times n} \tag{15}$$

The rows of P are unit vectors $\mathbf{e} \in \Re^n$ with $e_i = 1$ if i is a measurement location. By defining $\tilde{D}_{hy} = PD_{hY}$, and $\tilde{D}_{hZ} = PD_{hZ}$, one obtains the requirement

$$\begin{aligned}\text{Cov}'_{hh} \equiv P\,\text{Cov}_{hh}\,P^T &= \tilde{D}_{hY}\,\text{Cov}_{YY}\,\tilde{D}^T_{hY} + \tilde{D}_{hZ}\,\text{Cov}_{ZZ}\,\tilde{D}^T_{hZ} \\ &\quad + \tilde{D}_{hZ}\,\text{Cov}_{ZY}\,\tilde{D}^T_{hY} + \tilde{D}_{hY}\,\text{Cov}_{YZ}\,\tilde{D}^T_{hZ} \\ &\stackrel{!}{=} \text{Cov}'_{hh|\text{measurement error},}\end{aligned} \tag{16}$$

with $\text{Cov}_{hh}|_{\text{measurement error}}$ denoting the measurement error covariance matrix. If the errors are not correlated, this matrix is of diagonal form. In practical applications one can interpret the deviations between model output and measurement values as a combined model and measurement error σ_h. It is in this way that a "goodness of fit" criterion enters the conditional first-order second-moment method.

[23] Equation (16) can be solved exactly for Cov_{ZZ} if the number of head measurements N_h is equal to the number of parameters whose uncertainty range is to be estimated. If N_h is greater than N_Z, the system is overdetermined, and (16) can only be fulfilled in a least squares sense. In that case, Cov_{ZZ} must be determined in a way such that $\|\text{Cov}'_{hh} - \text{Cov}_{hh|\text{measurement error}}\|_2$ is minimal (where $\|\ \|_2$ denotes the square norm of a matrix):

$$\left\|\text{Cov}'_{hh} - \text{Cov}_{hh\,|\text{measurement error}}\right\|_2 \rightarrow \min. \tag{17}$$

If the uncertainty range of log recharge Z is of interest, (16) can be solved for Cov_{ZZ}:

$$\begin{aligned}\text{Cov}_{ZZ} = \left(\tilde{D}^T_{hZ} \cdot \tilde{D}_{hZ}\right)^{-1} \cdot \tilde{D}^T_{hZ} \cdot \left(\text{Cov}_{hh}|_{\text{measurement error}} - \tilde{D}_{hY} \cdot \text{Cov}_{YY}\right. \\ \left. \cdot \tilde{D}^T_{hY} - \tilde{D}_{hZ} \cdot \text{Cov}_{ZY} \cdot \tilde{D}^T_{hY} - \tilde{D}_{hY} \cdot \text{Cov}_{YZ} \cdot \tilde{D}^T_{hZ}\right) \\ \cdot \tilde{D}_{hZ} \cdot \left(\tilde{D}^T_{hZ} \cdot \tilde{D}_{hZ}\right)^{-1}.\end{aligned} \tag{18}$$

The residual of (17) is then minimal, because Cov_{ZZ} is obtained by solving the normal equations of a regression problem [*Golub and Van Loan*, 1996]. In case there are less head measurements than zones, that is, the model is overparameterized, the system of equations is undetermined, and no regression is possible.

[24] The expression for Cov_{ZY} in (18) can be derived by (13) and (5), finally leading to

$$\text{Cov}_{ZY} = -\left(\tilde{D}^T_{hZ} \cdot \tilde{D}_{hZ}\right)^{-1} \cdot \tilde{D}^T_{hZ}\,\tilde{D}_{hY} \cdot \text{Cov}_{YY}. \tag{19}$$

For each value of log hydraulic conductivity Y that lies within its certainty range (given by the trace Cov_{YY}), there will be a value of log recharge Z within its uncertainty range (given by the trace Cov_{ZZ}) that ensures that the model output at the measurement points will remain the same. Equation (18) quantifies this interdependence of the uncertainty ranges of log transmissivity Y and log recharge Z. This is the principle of interdependent uncertainty.

[25] Similarly to the derivation of Cov_{ZZ}, the uncertainty range of log hydraulic conductivity Y, Cov_{YY}, at given Cov_{ZZ} can be derived. Concentration measurements can likewise be used in conditioning the uncertainty range of either Cov_{ZZ} or Cov_{YY}. Similarly to the relation between Cov_{ZZ} and Cov_{ZY} for given head measurements, relations on the basis of concentration measurements can be deduced. The uncertainty range of log recharge Z for given concentration measurements and uncertainty in log transmissivity Y can be evaluated as

$$\begin{aligned}\text{Cov}_{ZZ} = \left[\left(\tilde{D}_{cZ} + \tilde{D}_{ch} \cdot D_{hZ}\right)^T \cdot \left(\tilde{D}_{cZ} + \tilde{D}_{ch} \cdot D_{hZ}\right)\right]^{-1} \cdot \left(\tilde{D}_{cZ} + \tilde{D}_{ch}\right. \\ \left. \cdot D_{hZ}\right)^T \cdot \left(\text{Cov}_{cc}|_{\text{measurement error}} - \tilde{D}_{cY} \cdot \text{Cov}_{YY} \cdot \tilde{D}^T_{cY}\right.\end{aligned}$$

$$
\begin{aligned}
&-\tilde{D}_{cY}\cdot \mathrm{Cov}_{YZ}\cdot \tilde{D}^T_{cZ} - \tilde{D}_{cZ}\cdot \mathrm{Cov}_{ZY}\cdot \tilde{D}^T_{cY}\\
&-\tilde{D}_{ch}\cdot D_{hY}\mathrm{Cov}_{YY}\cdot D^T_{hY}\cdot \tilde{D}^T_{ch} - \tilde{D}_{ch}\cdot D_{hZ}\mathrm{Cov}_{ZY}\cdot D^T_{hY}\cdot \tilde{D}^T_{ch}\\
&-\tilde{D}_{ch}\cdot D_{hY}\cdot \mathrm{Cov}_{YZ}\cdot D^T_{hZ}\cdot \tilde{D}^T_{ch}\\
&-\tilde{D}_{cY}\cdot \mathrm{Cov}_{Yh}\cdot \tilde{D}^T_{ch} - \tilde{D}_{ch}\cdot \mathrm{Cov}_{hY}\cdot \tilde{D}^T_{cY}\\
&-\tilde{D}_{cZ}\cdot \mathrm{Cov}_{ZY}\cdot D^T_{hY}\cdot \tilde{D}^T_{ch} - \tilde{D}_{ch}\cdot D_{hY}\cdot \mathrm{Cov}_{YZ}\\
&\cdot \tilde{D}^T_{cZ}\big)\cdot \big(\tilde{D}_{cZ}+\tilde{D}_{ch}\cdot D_{hZ}\big)\cdot \big[\big(\tilde{D}_{cZ}+\tilde{D}_{ch}\cdot D_{hZ}\big)^T\\
&\cdot \big(\tilde{D}_{cZ}+\tilde{D}_{ch}\cdot D_{hZ}\big)\big]^{-1}, \qquad (20)
\end{aligned}
$$

with Cov_{ZY} given by

$$
\begin{aligned}
\mathrm{Cov}_{ZY} = -\Big[\big(\tilde{D}_{cZ}+\tilde{D}_{ch}\cdot D_{hZ}\big)^T\cdot\big(\tilde{D}_{cZ}+\tilde{D}_{ch}\cdot D_{hZ}\big)\Big]^{-1}\\
\cdot\big(\tilde{D}_{cZ}+\tilde{D}_{ch}\cdot D_{hZ}\big)^T\big(\tilde{D}_{cY}+\tilde{D}_{ch}\cdot D_{hY}\big)\mathrm{Cov}_{YY}. \qquad (21)
\end{aligned}
$$

Equations (20) and (21) again relate the covariances of Cov_{YY} and Cov_{ZZ} to each other, now expressing the principle of interdependent uncertainty in the presence of concentration measurements.

[26] In the Monte Carlo approach, the primary alternative to this approach, the incorporation of head or concentration information is much more tedious and costly: A conditional Monte Carlo simulation requires the application of the inverse method for each realization.

[27] The deviations between measured and computed values are not only due to measurement error but also to the inadequacy of the model. To the latter type of error, which arises, for example, from the limited validity of equations applied, the limited resolution of input parameters, or two-dimensional flow and transport approximation, we refer to as "model error" in this work. Everything said above about measurement error can therefore be extended to model error. Since the model error could be spatially correlated, $\mathrm{Cov}_{hh|\text{measurement/model error}}$ would be a full matrix.

2.3. Limitations of the Method

[28] The FOSM method has two main limitations. First, the size of the covariance matrices can become infeasibly large as the number of nodes in the model becomes large. Owing to this limitation, realistic calculations are at present confined to steady state models of flow and transport. In time varying computations the large $n \times n$ matrices Cov_{hh} and Cov_{cc} have to be propagated at each time step, diminishing the computational efficiency relative to alternatives such as the Monte Carlo method. The limitation to steady state situations for piezometric heads and solute concentrations restricts the range of applications for which the FOSM method in its presented formulation can be used. However, important tasks remain where this limitation does not matter. One is the application of the FOSM method to the determination of stochastic wellhead protection zones [*Kunstmann et al.*, 1998; *Kunstmann*, 1998]. Another feasible application is the estimation of the uncertainty range of aquifer parameters such as groundwater recharge by conditioning with steady state environmental tracer data, as described in this paper.

[29] Second, uncertainty in parameters must be moderate, as the method is inherently a linear method.

[30] The first limit can partly be overcome by the efficient multiplication of matrices. At present, the number of nodes can be as much as several thousand nodes, which is sufficient for two-dimensional case studies.

[31] An extension of the Taylor series expansion to second-order terms, in principle, can improve the restriction on the limited variability of aquifer parameters. Such an extension yields the second-order second-moment method. The computationally efficient calculation of second derivatives, however, is cumbersome to realize in a computer code.

3. Application

3.1. Background

[32] The conditional FOSM method is now applied to an aquifer in semiarid Botswana. The code UFLOW [*Kunstmann*, 1998] contains all relevant routines of the theory presented and additionally the algorithms for the corresponding Monte Carlo simulations. This allows the comparison of the conditional FOSM method with inverse stochastic modeling by Monte Carlo simulations.

[33] The future water supply of Gaborone, the capital of Botswana, is to be ensured by the construction of the North-South Water Carrier. Once finished, water will be collected in a dam in the northeastern part of the country and transported over ~300 km to the city by means of a pipeline. If the system fails, either because of lack of water in the dam or technical problems with the pumping system, backup solutions based on groundwater resources are required. Several aquifers between Gaborone and Francistown have been investigated in terms of their potential yields. The groundwater abstraction potential of the Ntane sandstone aquifer in the Palla Road area (see Figure 1) is considered here [see also *Siegfried and Kinzelbach*, 1997]. Sustainability in the context of groundwater resources management requires that extractions from the aquifer do not exceed natural replenishment over a prolonged time period. The concept allows overdraft if a recovery period is subsequently granted to meet the equilibrium condition in the long run. Since the recharge rate is of major importance for the long-term extraction capacity, sustainable groundwater management requires quantification of its uncertainty bounds:

$$q_{\text{recharge}} = \hat{q}_{\text{recharge}} \pm \sigma_{\text{recharge}} \qquad (22)$$

or, if the recharge is assumed to be lognormally distributed, with $Z = \ln q_{\text{recharge}}$,

$$Z = \hat{Z} \pm \sigma_Z. \qquad (23)$$

Once the uncertainty bounds of q_{recharge} are quantified, conservative and sustainable decisions can be made.

3.2. Hydrogeological Setting of the Palla Road Aquifer

[34] Kalahari beds of variable thickness (up to 40 m) cover the model area and together with the several underlying layers described below constitute the Palla Road Aquifer. These deposits tend to thicken toward the center of the Kalahari basin situated to the west. They consist of unconsolidated aeolian sands, which commonly are calcretized or silcretized. In areas with extensive calcretization, such as pan structures, total dissolved solids (TDS) measurements of shallow groundwater confirm that substantial groundwater replenishment (i.e., >1 mm yr^{-1}) is restricted to areas with little calcretization [*Moehadu*, 1997]. Below the Kalahari beds a basalt layer of variable thickness extends under ~75% of the area. The variability of the thickness is related to intensive faulting as well as to the unevenness of the topography on which the lava was extruded. The basalt cover tends to thicken toward the west. Groundwater recharge potential increases where the basalt layer is thinner and where the basalt is fractured. The underlying Lebung formation consists of an aquitard (Mosolotsane siltstones) and the Ntane sandstone aquifer. The Mosolotsane siltstone shows a gradual transition into the predominantly sandy Ntane, which occasionally contains lenses of

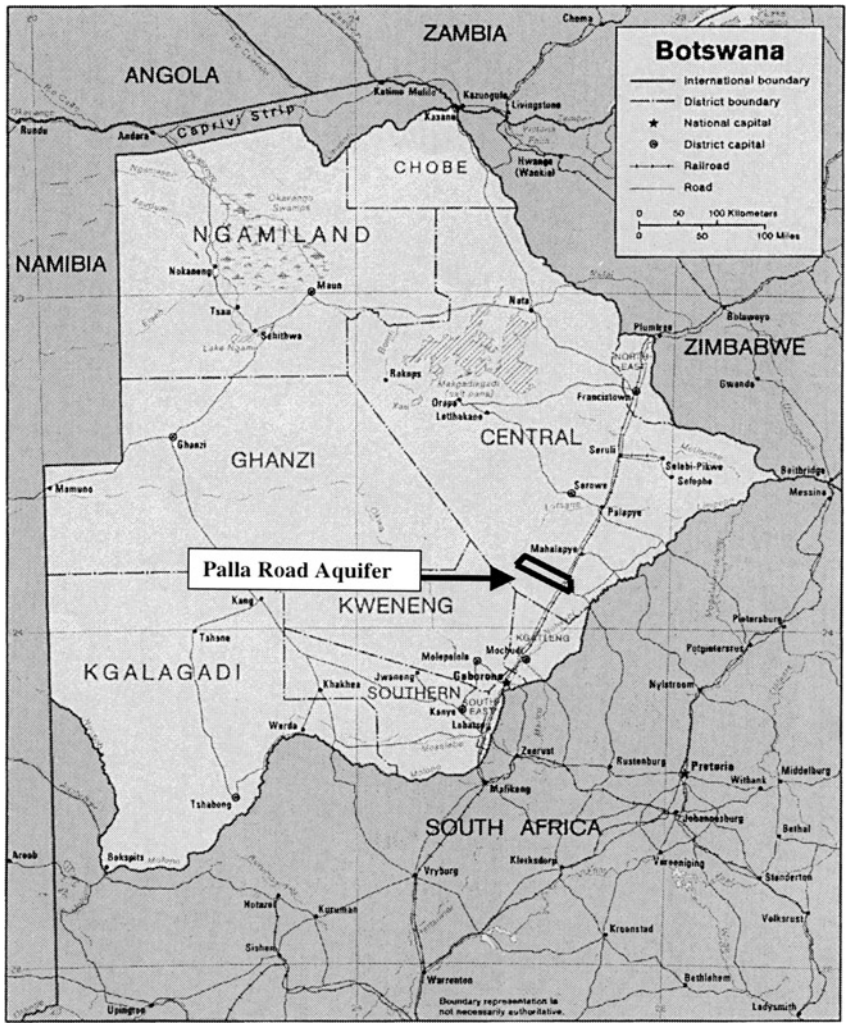

Figure 1. Site location of the Palla Road Aquifer.

siltstone. The Mosolotsane siltstone formation acts as a hydraulic boundary between the underlying highly saline Ecca sandstone aquifer and the Ntane freshwater aquifer. However, there are locations where the Ecca sandstone is shifted against the Ntane sandstone or where a hydraulic connection between the two aquifers is established because of a structural weakness of the Mosolotsane formation. In these locations, contamination of Ntane water with the saline Ecca waters occurs. Transport modeling of TDS concentration will address this concern. The Ntane sandstone outcrops between the Palla Road wellfield (in the southeastern quadrant of the model grid, see Figure 2) and the Kadimotse fault where the basalt cover is missing (~25% of the model area). The excellent water quality found in the Palla Road wellfield is related to a strongly increased recharge in this outcrop area.

[35] Estimates of mean recharge values were made using the soil chloride method [*Gieske*, 1992], which was first introduced by

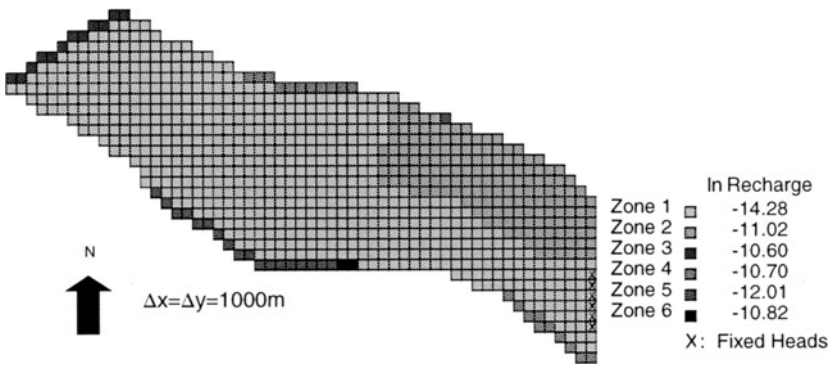

Figure 2. Six recharge and lateral inflow zones of the Palla Road Aquifer with log recharge q in ln(m d^{-1}) were chosen. Fixed-head cells are indicated also.

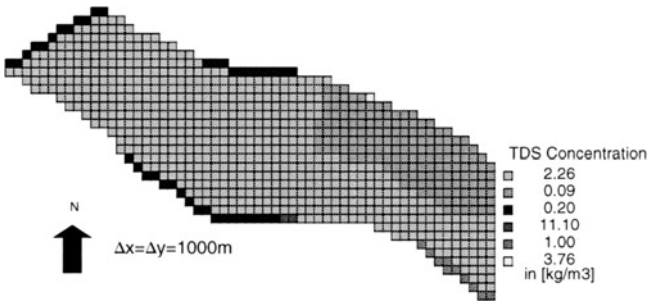

Figure 3. Total dissolved solids (TDS) concentration of inflows in kg m^{-3}.

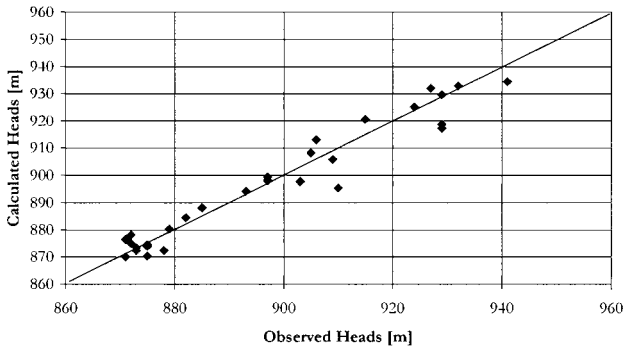

Figure 5. Scatterplot of observed heads versus calculated heads.

Eriksson and Khunakasem [1969]. Evaporation and recharge rates are estimated by determining the ratio of average chloride content in precipitation to that in groundwater. This technique has been used to evaluate recharge in a range of environments [*Allison and Hughes*, 1978; *Edmunds and Walton*, 1980; *Sharma and Hughes*, 1985; *Gieske*, 1992; *Wood and Sanford*, 1995]. Reviews of the method are given by *Simmers* [1988] and *Lerner et al.* [1990].

3.3. Model Layout and Boundary Conditions for the Palla Road Aquifer

[36] The model area extends over 57 km in the east-west direction and 34 km from northeast to southeast. The total head difference over the length of the aquifer is ~100 m. The spatial discretization lengths Δx and Δy were chosen as 1000 m [*Siegfried and Kinzelbach*, 1997]. The aquifer was assumed to be confined with aquifer thickness estimated from borehole logs [*Wellfield Consulting Services*, 1994]. Longitudinal dispersivity α_L was estimated to be 1 km, and transversal dispersivity α_T was set to 100 m.

[37] The recharge pattern was divided into six different zones. These groundwater recharge zones are assumed to represent areas with uniform recharge rates, with values that are uncertain and have a lognormal distribution. In the following the six zones of log recharge Z are summarized in the log recharge vector $\mathbf{Z} \in \Re^6$. The recharge zonation and the locations of the lateral inflows and their corresponding values are shown in Figure 2. Zone 1 covers the largest part of the model region and encompasses the area where the Ntane sandstone is covered with Stromberg lava. Recharge is highest in the Ntane sandstone outcrop areas (zone 2, in the northeast of the model area). Boundary fluxes were estimated from the area of the catchments draining into each boundary segment using areal recharge rates from information provided by *Wellfield Consulting Services* [1994].

[38] Zone 4 accounts for the contamination of the Ntane water by groundwater originating from the Ecca aquifer (Ecca-Saltwater Intrusion). Assuming proportionality between chloride and TDS concentration, the TDS concentrations of inflows shown in Figure 3 can be estimated using the soil chloride method [see *Siegfried and Kinzelbach*, 1997].

[39] The only outflow from the model area is on the southeastern edge. It was modeled by a fixed-head boundary (see Figure 2), since in the prepumping steady state situation the boundary always was on outflow boundary.

[40] *Siegfried and Kinzelbach* [1997] developed a deterministic flow and transport model adjusting the hydraulic conductivities such that simulated heads and chloride concentrations matched observations, assuming that recharge data were more reliable than conductivity data. Recharge estimates could be justified by both flow and salinity conditions, while the conductivities were only known as point values from pumping test sites, which are not representative of mean values for the zones used. Steady state calibration attempted to match observed heads in 1992, the first year with sufficient data. A cone of depression resulting from groundwater extraction in the Palla Road wellfield had at that time not yet spread, and extraction could be neglected. The hydraulic conductivity distribution was divided into three zones, based on geological structures following fault lines and a paleochannel structure along the centerline of the aquifer. The model parameter values were calibrated by taking into account both piezometric head and TDS concentration measurements.

[41] The calibrated zones of log hydraulic conductivity $Y' = \ln k_f$, with zonal parameters, are shown in Figure 4. In the following the three zones of log hydraulic conductivity Y are summarized in the vector $\mathbf{Y}' \in \Re^3$. On the basis of these mean parameters, flow and solute transport can be simulated. The good correspondences between observed and calculated heads and concentrations are illustrated in Figures 5 and 6, respectively.

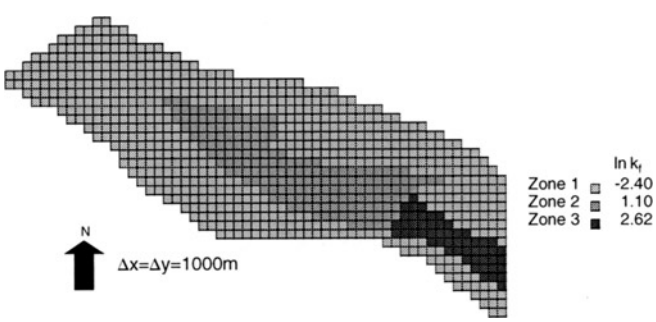

Figure 4. The ln k_f zones, k_f given in m d^{-1}.

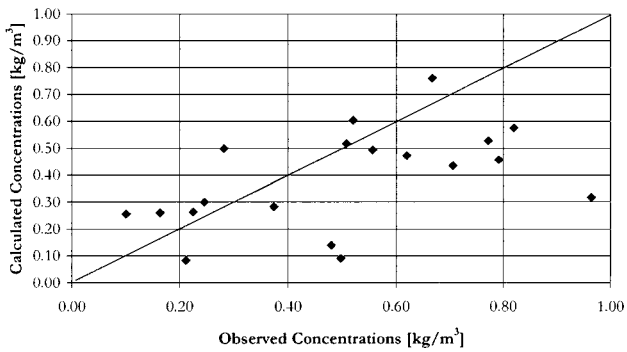

Figure 6. Scatterplot of observed concentrations versus calculated concentrations.

[42] The correlation between observed and calculated concentrations is less satisfactory than for heads. The deviations are due to the simplification of the natural system by choosing a two-dimensional model with a very limited number of free parameters. Calculations yield an integral value over the whole depth not accounting for the actual salinity profile. Little knowledge on the situation at the boundary is available. Also, salinity intrusion from the Ecca aquifer into some boreholes may be contaminating some observations [*Siegfried and Kinzelbach*, 1997].

[43] The fitted values of hydraulic conductivity k_f and the assumed values for groundwater recharge q are only one set of parameters that can satisfy observed head and concentration measurements. In terms of the sustainability constraint it is therefore vital to quantify the uncertainty range of groundwater recharge associated with the nonuniqueness of the solution of the inverse problem as well as with the quality of the data.

3.4. Corresponding Monte Carlo Simulation

[44] In the following the conditional FOSM method is compared to inverse stochastic modeling by conditional Monte Carlo simulations. The comparisons, for simplicity, will first assume that there are no model and measurement errors (i.e., $\mathrm{Cov}_{hh}|_{\text{model/measurement error}}$ = null matrix). The uncertainty of the log hydraulic conductivity, as estimated by pumping test analysis, is used to deduce the FOSM interdependent uncertainty of log recharge Z, according to (18), and (20). Section 3.5 describes how a Monte Carlo simulation is performed that corresponds to the conditional FOSM method so that a comparison of the two methods is possible.

[45] A conditional Monte Carlo simulation generates realizations of log hydraulic conductivity according to an assumed covariance structure. Then, for each log hydraulic conductivity realization the parameters of log recharge are fitted such that the weighted least squares deviation χ^2 between measured and modeled values of piezometric heads is minimized. The example discussed assumes that the uncertainties of the three zones of hydraulic conductivity are uncorrelated; the matrix Cov_{YY} is therefore diagonal. Random realizations of log hydraulic conductivity Y can be generated by Cholesky decomposition [*Press et al.*, 1992] of the covariance matrix Cov_{YY}, following *Robin et al.* [1993], for any given covariance structure. Details are given by [*Kunstmann*, 1998]. When Cov_{YY} is diagonal, the decomposition is trivial.

[46] For each realization v of log hydraulic conductivity Y the flow model must be run in inverse mode to fit the corresponding log recharges Z,

$$ {}^{v}\mathbf{Y}_{\text{random}},\ {}^{v}\chi^2 = \sum_{i=1}^{N} \frac{\left(h_{\text{modeled},i} - h_{\text{observed},i}\right)^2}{\sigma_{h_i}^2} \rightarrow \min, \quad \Rightarrow {}^{v}\mathbf{Z}_{\text{estimated}}. \tag{24} $$

This minimization was accomplished here by application of the Marquardt-Levenberg algorithm [*Press et al.*, 1992] to each realization of Y. Convergence of first and second moments of concentrations in the Monte Carlo approach is checked by monitoring the evolution of the average-per-node (APN) first and second moment of TDS concentration as N'_{MC} is increased:

$$ \hat{c}_{\mathrm{APN}}\left(N'_{\mathrm{MC}}\right) = \frac{1}{n} \sum_{j,i \in \text{grid}} \hat{c}_{j,i}\left(N'_{\mathrm{MC}}\right) \tag{25} $$

$$ \sigma^2_{c_{\mathrm{APN}}}\left(N'_{\mathrm{MC}}\right) = \frac{1}{n} \sum_{j,i \in \text{grid}} \sigma^2_{\hat{c}_{j,i}}\left(N'_{\mathrm{MC}}\right). \tag{26} $$

Table 1. Mean and Standard Deviation of $\ln k_f$ for the Three Hydraulic Conductivity Zones as Used in the Comparison Between Conditional FOSM Method and Conditional Monte Carlo Method[a]

Zone	Mean $\ln k_f$	Sigma $\ln k_f$	Mean k_f	Sigma k_f
1	−2.40	0.40	0.09	0.04
2	1.10	0.40	2.99	1.25
3	2.62	0.20	13.79	2.79

[a] Here k_f is given in m d^{-1}.

N'_{MC} denotes the number of Monte Carlo realizations performed at which (25) and (26) are evaluated; n denotes the total number of nodes. In addition, the mean and the variance of the zonal values of the generated log hydraulic conductivity Y and the fitted log recharge Z are calculated.

[47] In steady state situations (as in the case study discussed) the Marquardt-Levenberg algorithm requires estimates of the sensitivities $\partial h/\partial p$; in this application the sensitivities were determined by direct derivation from the model equations (see *Kunstmann* [1998] for details). If the parameters to be estimated are the log recharge Z, the sensitivities required by the Marquardt-Levenberg algorithm are the entries of the sensitivity matrix D_{hZ}

$$ \frac{\partial h_{\text{modeled},i}}{\partial Z_k} = D_{hZ}\big|_{l \hat{=} i,k} \tag{27} $$

introduced in (4), (5), and (6). The CPU time savings by the direct evaluation of these sensitivities are enormous. The conditional Monte Carlo method used in this study is therefore already computationally more efficient than one based on sensitivity calculations that use a secant approximation [*Yeh*, 1986]. Nevertheless, the conditional Monte Carlo method is still computationally more demanding than the conditional FOSM method, as shown in section 3.5.

3.5. Comparison Between Conditional FOSM Method and Conditional Monte Carlo Simulation

[48] In the following analysis, $Z' = \ln Q = \ln(q\Delta x\Delta y)$ is used as the variable describing recharge instead of $Z = \ln q$. With given head measurements and for a given level of uncertainty in log hydraulic conductivity Y (Table 1), the conditional FOSM method first calculates the mixed covariances $\mathrm{Cov}_{Z'Y}$ and $\mathrm{Cov}_{YZ'}$ (equation (19)) and then the uncertainty of Z', expressed through its covariance matrix $\mathrm{Cov}_{Z'Z'}$ (equation (18)). These uncertainties then are propagated into estimates of piezometric head and solute concentration uncertainty (equations (4) and (10)).

[49] For the purpose of investigating the equivalence between the FOSM and Monte Carlo methods the uncertainty range of $Y = \ln k_f$ is chosen such that the first-order approximation of the FOSM method is valid. Ten head measurements were selected for the inverse stochastic analysis of the Palla Road Aquifer. Four out of the 10 were interpolated since there was not a measurement available in each zone of groundwater recharge. The four synthetic head measurements will be replaced by real head measurements, and a larger Cov_{YY} will be used in section 3.6.

[50] Our assumption of no model and measurement errors means that the fitting of recharge values for each realization of the Monte Carlo simulation is performed with the head values calculated by the mean model parameters, $\hat{\mathbf{Y}}$ and $\hat{\mathbf{Z}}'$, instead of the real head measurements. This approach is necessary to be fully compatible with the conditional FOSM method in the formulation that does not include model and measurement errors. The deviation

Table 2. Comparison of Mean $\hat{Z}'$ and Standard Deviation Sigma Z' as Calculated by the Monte Carlo and the FOSM Methods[a]

Zone	MONTE CARLO		FOSM	
	Mean Z'	Sigma Z'	Mean Z'	Sigma Z'
1	−0.58	0.78	−0.47	1.21
2	2.77	0.30	2.80	0.35
3	3.13	0.32	3.21	0.59
4	3.03	0.26	3.11	0.22
5	1.73	0.29	1.81	0.32
6	2.76	0.81	3.00	0.98

[a] $Z' = \ln(Q)$, $Q = (q\Delta x\Delta y)$, and recharge q is given in m d^{-1}.

of measured heads from the average computed heads is for our purposes primarily the model error that will be discussed in section 3.8 and section 3.9.

3.6. Comparison of Resulting Cov_{ZZ} Between FOSM and Monte Carlo Method

[51] As a check of the conditional FOSM method and the principle of interdependent uncertainty, we first compare the diagonal of $Cov_{Z'Z'}$ obtained by (18) with Monte Carlo statistics. FOSM conditional analysis gives the uncertainty of log recharge $Cov_{Z'Z'}$ for specified head measurements and specified $Cov_{YY'}$.

[52] The square roots of the diagonal elements of $Cov_{Z'Z'}$ from FOSM are compared to the log recharge rates fitted in the conditional Monte Carlo simulations in Table 2. The good correspondence between Monte Carlo and FOSM method results clearly shows the consistency of the proposed FOSM formulae. The calculated $Cov_{Z'Z'}$ is now inserted into the propagation of the head and concentration uncertainty, and the results are compared to the Monte Carlo method. The calculation of the covariance propagation of Cov_{hh} and Cov_{cc} is performed according to the expressions given in (4) and (10).

3.7. Comparison of First and Second Moments of Heads and TDS Concentrations

[53] The resulting mean piezometric head distribution is illustrated in Figure 7. Increased recharge is responsible for the steep gradients visible in the northeastern area, whereas higher effective conductivity in the graben structure to the south diminishes head gradients there. There is no difference in the results between FOSM and Monte Carlo approach, indicating that the first moment is not yet influenced by the parameter perturbation.

[54] The second moment of the piezometric head is illustrated in Figures 8 and 9. The first and second moments of heads from the FOSM and Monte Carlo results are satisfactorily similar. There are 10 local minima for the standard deviation of the heads in fact, exactly at the 10 measurement locations. These minima are smoothed in Figures 8 and 9 because of the interpolation applied. The minima would be exactly equal to zero if (16) could be solved exactly, that is, if the number of head measurements would be equal to the number of groundwater recharge zones. In the case of 10 head measurements and six groundwater recharge zones, as in the example presented, (16) can only be fulfilled in a least squares sense, yielding local minima of the heads' standard deviations at the measurement locations.

[55] Figure 10 shows the concentration distribution. The calculation confirms that the excellent water quality found in the Palla Road wellfield can be explained by the increased recharge in the area where the Ntane sandstone outcrops. The intrusion of low-quality water still represents the main threat to the Palla Road wellfield and is visible as a saltwater plume along the southern boundary of the aquifer. FOSM and Monte Carlo distributions of mean concentrations correspond well, indicating that the first moment of the TDS concentrations has also not been shifted by the parameter uncertainties.

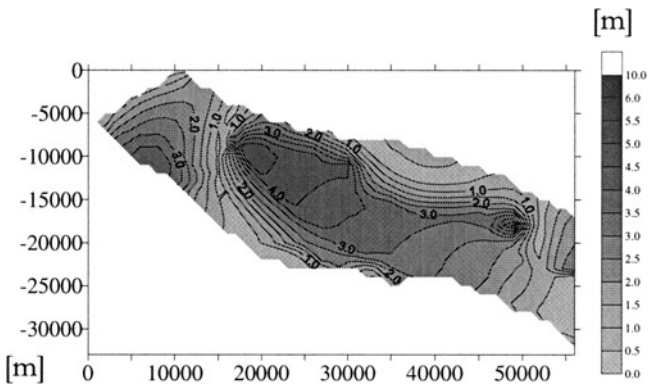

Figure 8. Standard deviations of heads in meters (FOSM method, Palla Road Aquifer, conditioned by 10 head measurements).

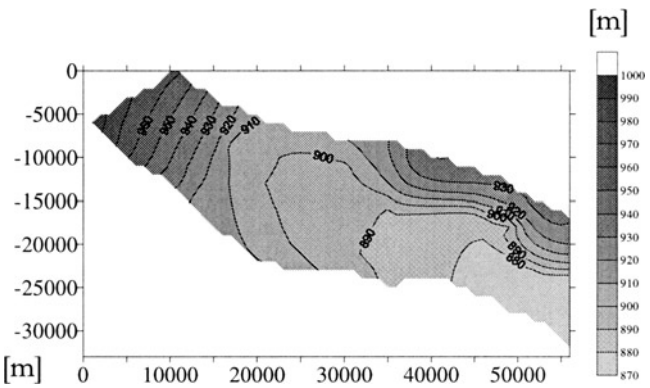

Figure 7. First moment of heads in meters (first-order second-moment (FOSM) method, Palla Road Aquifer, conditioned by 10 head measurements).

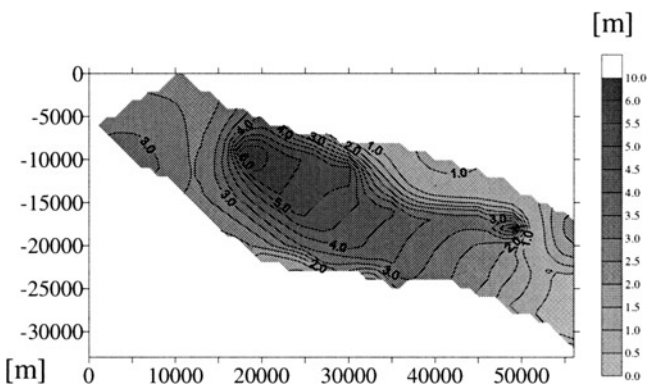

Figure 9. Standard deviations of heads in meters (Monte Carlo method, Palla Road Aquifer, conditioned by 10 head measurements).

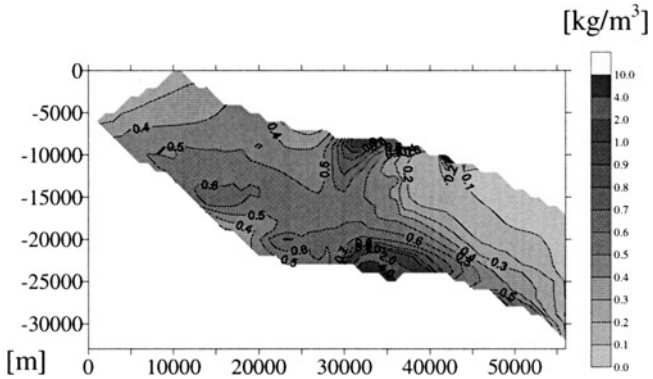

Figure 10. First moment of concentrations in kg m^{-3} (FOSM method, Palla Road Aquifer, conditioned by 10 head measurements).

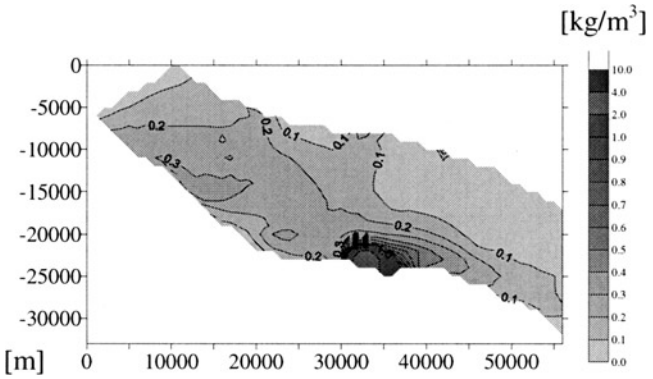

Figure 12. Standard deviations of concentrations in kg m^{-3} (Monte Carlo method, Palla Road, conditioned by 10 head measurements).

[56] Figures 11 and 12 show the standard deviations of TDS concentrations, conditioned by the 10 head measurements. The similarities between standard deviations from the FOSM method and Monte Carlo method are clearly visible. The FOSM standard deviation is larger in the southeastern region than in the Monte Carlo result.

[57] The convergence behavior of the Monte Carlo simulation, according to (25) and (26), is illustrated in Figure 13. About 500 realizations were sufficient to achieve convergence. Only 694 out of the 750 realizations of the Monte Carlo method were accepted to be included into the statistics since the χ^2 values of the remaining 56 realizations exceeded the specified threshold value. The FOSM method was ~35 times less demanding of CPU time than 500 Monte Carlo realizations and was 60 times less demanding than 750 Monte Carlo realizations. If the convergence control variables were normally distributed, one could give a priori estimates for the required number of Monte Carlo simulations for any desired confidence levels [e.g., *Bronstein et al.*, 1996].

[58] If one is only interested in the uncertainty range $Cov_{Z'Z'}$ (equation (18)) and not in the resulting uncertainty of the head or concentration distribution, Cov_{hh} (see Figures 8 and 9) and Cov_{cc} (see Figures 11 and 12), the FOSM method shows its largest advantage over the Monte Carlo method. In this case the propagation of large size covariance matrices required for obtaining Cov_{hh} and Cov_{cc} can be omitted in the FOSM method, whereas the Monte Carlo method still requires the time-consuming repeated solution of the system equations for the random realizations generated. The CPU time requirement for the calculation of standard deviations σ_z of the FOSM method alone (Table 2) is <1% of the Monte Carlo requirements.

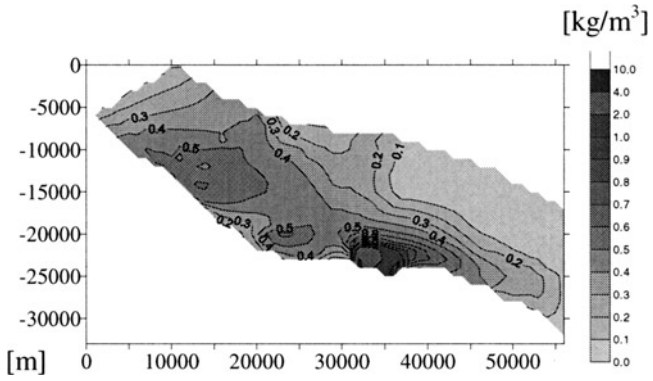

Figure 11. Standard deviations of concentrations in kg m^{-3} (FOSM method, Palla Road Aquifer, conditioned by 10 head measurements).

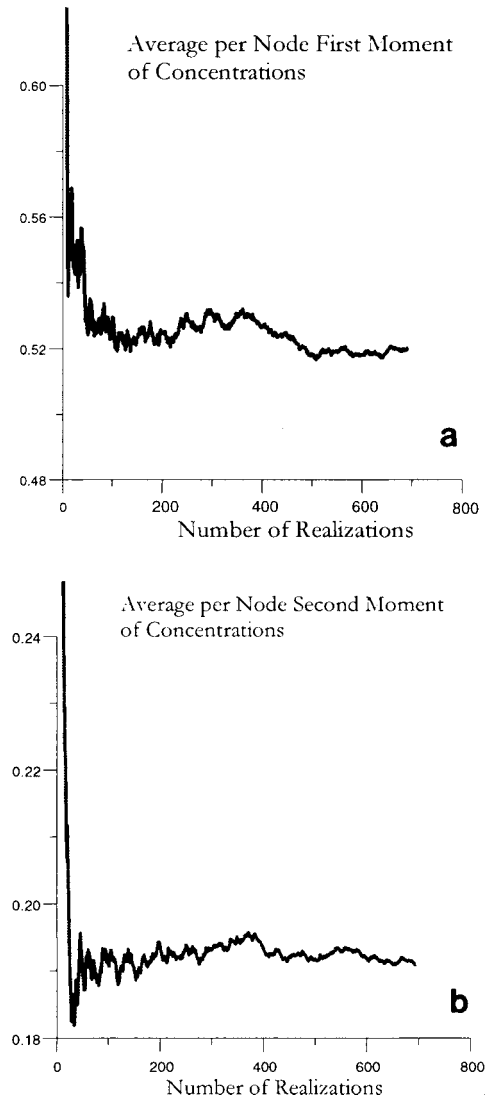

Figure 13. Convergence behavior of (a) first and (b) second moment of concentrations (Monte Carlo method, Palla Road Aquifer, conditioned by 10 head measurements).

Table 3. Uncertainty of Log Hydraulic Conductivity as Deduced From Pumping Test Analysis and as Used in the Estimation of the Uncertainty Range of Groundwater Recharge[a]

Zone	Mean $\ln k_f$	Sigma $\ln k_f$	Mean k_f	Sigma k_f
1	−2.40	1.00	0.09	0.12
2	1.10	1.00	2.99	3.92
3	2.62	0.50	13.79	7.35

[a] Here k_f is given in m d^{-1}.

3.8. Uncertainty Quantification of Groundwater Recharge by FOSM Conditional Analysis Under Field Conditions

[59] The actual uncertainties of the log hydraulic conductivity, $\ln k_f$, are probably larger than the ones assumed in Table 1. Additionally, four out of 10 head measurements were simulated rather than observed. This was done to attribute to each recharge zone at least one head measurement. These four simulated measurements are now replaced with real measurements (at real locations). On the basis of the pumping test data [*Siegfried and Kinzelbach*, 1997; *Wellfield Consulting Services*, 1994] the uncertainties of log hydraulic conductivity shown in Table 3 are assumed.

[60] The transformation of log normally distributed variables such as hydraulic conductivity k_f to normally distributed variables like $Y = \ln k_f$, and vice versa, is approximated by $\overline{Y}' = \ln \bar{k}_f$ and

$$\sigma^2_{Y'} = \ln\left[\frac{\sigma^2_{k_f}}{\bar{k}_f^2} + 1\right]$$

[e.g., *Hahn and Shapiro*, 1967]. This approximation neglects the influence of the perturbation of σ_{k_f} on the mean $\bar{Y}'$, which, in fact, is a first-order approximation.

[61] In the following, conditioning by head information is compared to conditioning by concentration information. The deviation between measurements and model output, described by the measurement error covariance matrix $\mathrm{Cov}_{hh}|_{\text{model/measurement error}}$ and $\mathrm{Cov}_{cc}|_{\text{model/measurement error}}$, respectively, now is included. We take the deviations between mean model output and measurement (illustrated in Figures 5 and 6, respectively) as square roots of the diagonal elements of $\mathrm{Cov}_{hh}|_{\text{model/measurement error}}$, $\mathrm{Cov}_{cc}|_{\text{model/measurement error}}$, respectively. Both $\mathrm{Cov}_{hh}|_{\text{model/measurement error}}$ and $\mathrm{CCov}_{cc}|_{\text{model/measurement error}}$ are assumed to be diagonal matrices for simplicity and for lack of correlation information.

3.9. Conditioning by 10 Head Measurements

[62] Applying the FOSM conditional analysis to the quantification of the recharge uncertainties under field conditions yields the results in Table 4. It can be seen that the uncertainty ranges of log recharge are rather large. This computation demonstrates that the conditional FOSM method is a quick and easy-to-use tool to examine whether a certain measurement location yields uncertainty reduction or not. The result indicates that there should be at least one head measurement for each log recharge zone to be estimated (as was the case in the derivation of the results in Table 2); future positioning of observation boreholes should address this concern.

Table 4. FOSM Means and Standard Deviations of $Z' = \ln(Q)$[a]

Zone	Mean Z'	Sigma Z'	Sigma Z'[b]
1	−0.47	5.79	13.36
2	2.80	1.02	1.04
3	3.21	2.32	5.00
4	3.11	1.51	2.09
5	1.81	7.71	10.03
6	3.00	90.58	117.90

[a] $Q = q\Delta x\Delta y$; recharge q in m d^{-1} is conditioned by 10 head measurements.
[b] Model error is included.

Table 5. FOSM Means and Standard Deviations of $Z' = \ln(Q)$[a]

Zone	Mean Z'	Sigma Z'[b]	Sigma Z' [c]	Mean q[c]	Sigma q[c]
1	−0.47	0.13	0.90	6.25E-07[d]	6.98E-07
2	2.80	0.07	0.44	1.64E-05	7.58E-06
3	3.21	0.30	1.90	2.48E-05	1.49E-04
4	3.11	0.19	0.40	2.25E-05	9.38E-06
5	1.81	0.12	2.00	6.10E-06	4.46E-05
6	3.00	0.28	1.00	2.00E-05	2.62E-05

[a] $Q = q\Delta x\Delta y$; recharge q in m d^{-1} is conditioned by 19 concentration measurements.
[b] Model error is not included.
[c] Model error is included.

3.10. Conditioned by 19 Concentration Measurements

[63] FOSM conditional analysis allows conditioning by concentration measurements. For given standard deviations of log hydraulic conductivity Y and concentration measurements, as well as the deviations of the model output from observations (described as $\mathrm{Cov}_{cc}|_{\text{model/measurement error}}$), the resulting standard deviations of the logarithm of the recharge flux, $Z' = ln(q\Delta x\Delta y)$, are given by (20). No comparison to Monte Carlo results will be given here since our code UFLOW [*Kunstmann*, 1998] does not yet include an inverse stochastic modeling tool for solute transport.

[64] If the standard deviation of log recharge is conditioned by concentration measurements instead of piezometric head measurements, the resulting uncertainty bounds are much smaller, as the values listed in Table 5 demonstrate. Table 5 also shows the uncertainties that are obtained when model error is included in the analysis. The fourth column shows the standard deviation of $Z' = \ln(q\Delta x\Delta y)$ including the model error; columns five and six show the corresponding values for mean groundwater recharge and its standard deviation.

[65] The difference between FOSM standard deviations of Z' from the calculations neglecting model errors and those that are including model errors is larger with the concentration observations than with head observations. This is because the piezometric heads were fitted more satisfactorily than the chloride concentrations.

Table 6. FOSM Uncertainty in Total Groundwater Recharge Rate for the Palla Road Aquifer

Zone	Area km^2	Total Q, m^3 d^{-1}	Sigma Q, m^3 d^{-1}
1	624	399	431
2	169	2773	1284
3	12	298	1680
4	21	473	210
5	19	116	855
6	2	40	360
Sum[a]	847	4100	2358

[a] Sum of sigma Q is the square root of the sum of the individual variances.

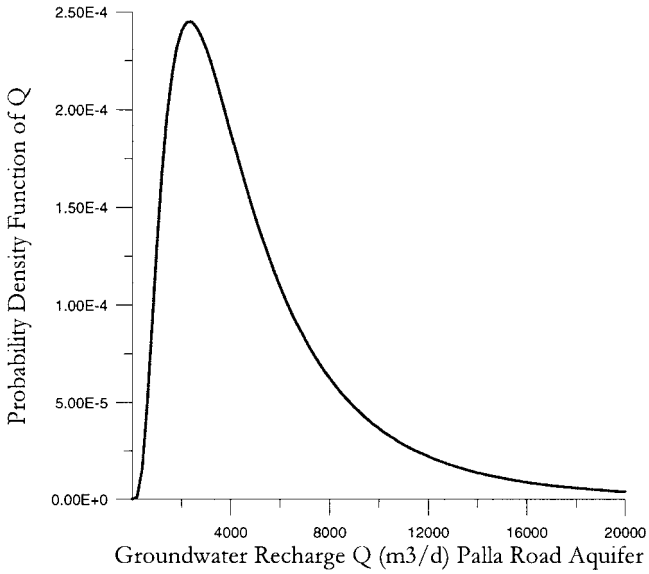

Figure 14. Probability density function of the groundwater recharge for the Palla Road Aquifer.

[66] The final estimates of σ_z include the uncertainties related to the nonuniqueness of the inverse problem and to the quality of fit of the measurements. In spite of the worse fit of the concentration measurements compared to the head measurements, the value of concentration measurements for conditioning is larger than the value of head information. This is due to the fact that concentrations reflect both mixing ratios and streamlines and therefore contain valuable information on fluxes, which would remain ambiguous with head information only.

[67] Thus greater emphasis on the measurement of environmental tracers may be warranted [see also *Kauffmann and Kinzelbach*, 1989; *Zoellmann and Kinzelbach*, 1996; *Plumacher and Kinzelbach*, 1998]. In settings such as the Palla Road Aquifer, the best information comes from environmental tracer concentrations. Generally, the relaxation times of heads are much smaller than the relaxation times of concentrations: The tracer concentration is assumed to reflect the history of the aquifer for the last 1000–4000 years, whereas the steady state head distribution probably reflects the past 50 years. Therefore care must be taken when comparing long-term average head to tracer information. The recharge information deduced from environmental tracers and from piezometric heads reflect two different timescales.

4. Conclusions for the Palla Road Aquifer

[68] The mean natural replenishment of the Palla Road aquifer is estimated to be 4100 $m^3\ d^{-1}$. The uncertainty of this value, as derived from the FOSM method conditioned by TDS measurements, is 2400 $m^3\ d^{-1}$ (Table 6).

[69] The probability density function of the resulting lognormally distributed recharge is illustrated in Figure 14. The derivation of Figure 14 includes the approximation that the sum of six independent lognormally distributed zonal recharge values is essentially lognormally distributed.

[70] In 1996, pumpage from the Palla Road wellfield was ~3100 $m^3\ d^{-1}$, which is also the long-term average value considered for future operation. The probability density function in Figure 14 shows the probability that the actual recharge is smaller that this pumpage rate, i.e., the failure probability of the management scheme:

$$\text{probability}\left(\text{actual recharge} < 3100\ m^3\ d^{-1}\right) = 30\%.$$

This failure probability is rather high. Moreover, the natural replenishment of the aquifer is the practical maximum amount of water that can theoretically be extracted. It does not yet include possible minimum outflow requirements for ecological reasons. Moreover, the calculated failure probability does not include uncertainties arising from possible climate change effects that are neglected in the soil chloride method. If the pumping was decreased to 2000 $m^3\ d^{-1}$, the failure probability would be reduced to 10%, and if it was decreased to 1000 $m^3\ d^{-1}$, the estimated failure probability would be reduced to 0.4%.

[71] The final estimation of the recharge uncertainty includes both the uncertainties related to the nonuniqueness of the inverse problem and the uncertainties related to the model/measurement errors. This may lead to a criterion for an optimal number of zones for hydraulic conductivity (or transmissivity) and recharge. An increased number of zones will improve the goodness of fit but increases the nonuniqueness of the result. A reduced number of zones worsens the goodness of fit but decreases the uncertainty related to the nonuniqueness of the inverse problem. The optimal number of zones would be the number that minimizes some joint uncertainty consisting of both $\mathrm{Cov}_{cc|\text{model/measurement error}}$ (or $\mathrm{Cov}_{hh|\text{model/measurement error}}$) and Cov_{ZZ} (at given a priori Cov_{YY}). The optimal number would depend on the model application and other conditions that will be recognizable only after many more settings are analyzed by the methods developed here.

5. Summary

[72] On the basis of a first-order Taylor series expansion the first-order second-moment (FOSM) method was extended and applied to the groundwater flow and solute transport equations in both unconditional and conditional analysis. The FOSM method is a fast and reliable method to estimate uncertainty of groundwater models. The two main limitations of the method are the size of the covariance matrices appearing and the restriction to moderate variability of parameters as it is inherently a linear method. Closed formulae obtained by the method clearly explain how conditioning information diminishes the uncertainty of the model output. The uncertainty arising from the nonuniqueness of the inverse problem is quantified. This principle of interdependent uncertainty shows how the uncertainties of hydraulic conductivity and groundwater recharge are related to each other in the presence of head or concentration measurements. In addition, the influence of model and measurement errors is quantified.

[73] We applied the conditional FOSM method and the principle of interdependent uncertainty to a field case study in Botswana. The objective was to quantify the exploitation potential of an aquifer in terms of its mean annual recharge and its uncertainty bounds. The results obtained by the FOSM method were compared with a corresponding Monte Carlo simulation, and the conditional FOSM method successfully reproduced the Monte Carlo result. The FOSM method, however, required 30–60 times less CPU time.

[74] The analysis for the Palla Road Aquifer revealed a failure probability for the present management scheme of at least 30%. It was demonstrated that the value of concentration measurements for conditioning is much larger than the value of head information.

This reflects the fact that concentrations imply mixing ratios and streamlines and therefore valuable information on fluxes, which would remain ambiguous with head information only. More emphasis therefore must be directed to the measurement of environmental tracers to supplement piezometric heads.

[75] **Acknowledgments.** The advice of Lloyd Townley at Townley & Associates Pty Ltd, Claremont, Australia, and helpful discussions with Dennis McLaughlin at MIT, Boston, USA, are gratefully acknowledged. The work on the Palla Road aquifer was only possible with the help of Geotechnical Consulting Services and the Department of Water Affairs, both in Gaborone, Botswana. Their contribution is also gratefully acknowledged.

References

Allison, G. B., and M. W. Hughes, The use of environmental chloride and tritium to estimate total recharge in an unconfined aquifer, *Aust. J. Soil Res.*, *16*, 181–195, 1978.

Ang, A. H. S., and W. H. Tang, *Probability Concepts in Engineering Planning and Design*, vol. II, *Decision, Risk and Reliability*, John Wiley, New York, 1984.

Bear, J., *Dynamics of Fluids in Porous Media*, Dover, New York, 1972.

Bronstein, I., K. Semendjajew, G. Grosche, V. Ziegler, and D. Ziegler, *Teubner Taschenbuch der Mathematik*, B. G. Teubner, Stuttgart, Germany, 1996.

Carrera, J., and S. Neumann, Estimation of aquifer parameters under transient and steady state conditions, 1, Maximum likelihood method incorporating prior information, *Water Resour. Res.*, *22*(2), 199–210, 1986.

Clifton, P. M., and S. P. Neumann, Effects of kriging and inverse modeling on conditional simulation of the Avra Valley aquifer in southern Arizona, *Water Resour. Res.*, *18*(4), 1215–1234, 1982.

Connell, L. D., An analysis of perturbation based methods for the treatment of parameter uncertainty in numerical groundwater models, *Transp. Porous Media*, *21*, 225–240, 1995.

Cooley, R. L., A method of estimating parameters and assessing reliability for models of steady state groundwater flow, 2, Application of statistical analysis, *Water Resour. Res.*, *15*(3), 603–617, 1979.

Dagan, G., Analysis of flow through heterogeneous random aquifers, 2, Unsteady flow in confined formations, *Water Resour. Res.*, *18*(5), 1571–1585, 1982.

Delhomme, J. P., Spatial variability and uncertainty in groundwater flow parameters, A geostatistical approach, *Water Resour. Res.*, *15*(2), 269–280, 1979.

Dettinger, M., Numerical modeling of aquifer system under uncertainty: A second moment analysis, M. Sci. thesis Dep. of Civ. Eng., Mass. Inst. of Technol., Cambridge, 1979.

Dettinger, M. D., and J. L. Wilson, First order analysis of uncertainty in numerical models of groundwater flow, 1, Mathematical development, *Water Resour. Res.*, *17*(1), 149–161, 1981.

Devary, J. L., and P. G. Doctor, Pore velocity estimation uncertainties, *Water Resour. Res.*, *18*(4), 1157–1164, 1982.

Edmunds, W. M., and N. R. G. Walton, A geochemical and isotopic approach to recharge evaluation in semi-arid zones—Past and present, in *Arid Zone Hydrology: Investigations With Isotope Techniques*, *Rep. 47–68*, Int. At. Energy Agency, Vienna, 1980.

Eriksson, E., and V. Khunakasem, Chloride concentration in groundwater, recharge rate and rate of deposition of chloride in the Israel coastal plain, *J. Hydrol.*, *7*, 178–197, 1969.

Gelhar, L. W., *Stochastic Subsurface Hydrology*, Prentice-Hall, Englewood Cliffs, N. J., 1993.

Gieske, A., *Dynamics of Groundwater Recharge, A Case Study in Semi-Arid Eastern Botswana*, Acad. Proefschr., Enschede, Netherlands, 1992.

Golub, G. H., and C. F. Van Loan, *Matrix Computations*, 3rd ed. John Hopkins Univ. Press, Baltimore, Md., 1996.

Graham, W., and D. McLaughlin, Stochastic analysis of nonstationary subsurface solute transport, 1, Unconditional moments, *Water Resour. Res.*, *25*(1), 215–232, 1989a.

Graham, W., and D. McLaughlin, Stochastic analysis of nonstationary subsurface solute transport, 2, Conditional moments, *Water Resour. Res.*, *25*(11), 2331–2355, 1989b.

Hahn, G. J., and S. S. Shapiro, *Statistical Models in Engineering*, John Wiley, New York, 1967.

Hamed, M. M., J. P. Conte, and P. B. Bedient, Probabilistic screening tool for groundwater contamination and risk assessment, *J. Environ. Eng.*, *121*(11), 767–775, 1995.

Hoeksema, R. J., and P. K. Kitanidis, Comparison of Gaussian conditional mean and kriging estimation in the geostatistical solution of the inverse problem, *Water Resour. Res.*, *21*(6), 825–836, 1985.

James, A. L., and C. M. Oldenburg, Linear and Monte Carlo uncertainty analysis for subsurface contaminant transport simulation, *Water Resour. Res.*, *33*(11), 2495–2508, 1997.

Kauffmann, C., and W. Kinzelbach, Parameter estimation in contaminant transport modelling, in *Contaminant Transport in Groundwater*, edited by H. Kobus, and W. Kinzelbach, A. A. Balkema, Brookfield, Vt., 1989.

Kunstmann, H., Computationally efficient methods for the quantification of uncertainties in groundwater modeling, *Diss. ETH 12722*, Inst. für Hydromech. und Wasserwirt. Eidg. Tech. Hochsch. Zürich, Zürich, Switzerland, 1998.

Kunstmann, H., and W. Kinzelbach, Computation of stochastic wellhead protection zones by combining the first-order second-moment method and Kolmogorov backward equation analysis, *J. Hydrol.*, *237*, 127–146, 2000.

Kunstmann, H., W. Kinzelbach, and G. van Tonder, Groundwater resources management under uncertainty, paper presented at XII International Conference on Computational Methods in Water Resources, Inst. of Chem. Eng. and High Temp. Chem. Processes — Found. for Res and Technol., Crete, Greece, June 1998.

Lerner, D. N., A. S. Issar, and I. Simmers, Groundwater recharge, A guide to understanding and estimating natural recharge, *Int. Contrib. Hydrogeol.*, vol. 8, Heinz Heise, Hannover, Germany, 1990.

Madsen, H., S. Krenk, and N. C. Lind, *Methods of Structural Safety*, Prentice-Hall, Englewood Cliffs, N. J., 1986.

McLaughlin, D. B., and E. F. Wood, A distributed parameter approach for evaluating the accuracy of groundwater model predictions, 1, Theory, *Water Resour. Res.*, *24*(7), 1037–1047, 1988.

Moehadu, O. M., *GIS Based Groundwater Recharge Potential Evaluation — A Case Study at Khurutshe, "Kgatleng/Central District", Botswana,*, Int. Inst. for Aerospace SUW. and Sci., (ITC), Enschede, Netherlands, 1997.

Plümacher, J., and W. Kinzelbach, Regionale Stromungs- und Transportmodellierung zur Ermittlung des Einzugsgebiets der Mineralquellen von Stuttgart - Bad Cannstatt, in Das Stuttgarter Mineralwasser—Herkunft und Genese, edited by W. T. Ufrecht and G. Einsele, no. 1, pp. 117–137, Schriftenreihe des Amtes fur Umweltschutz, Stuttgart, Germany, 1998.

Press, W. H., S. A. Teukolsky, W. T. Vetterling, and B. P. Flannery, *Numerical Recipes in C, The Art of Scientific Computing*, 2nd ed., Cambridge Univ. Press, New York, 1992.

Robin, M. J. L., A. L. Gutjahr, E. A. Sudick, and J. L. Wilson, Cross-correlated random field generation with the direct Fourier transform method, *Water Resour. Res.*, *29*(7), 2385–2397, 1993.

Scheidegger, A. E., General theory of dispersion in porous media, *J. Appl. Phys.*, *25*(8), 994–1001, 1961.

Sharma, M. L., and M. W. Hughes, Groundwater recharge estimation using chloride, deuterium and oxygen-18 profiles in the deep coastal sands of Western Australia, *J. Hydrol.*, *81*, 93–109, 1985.

Siegfried, T., and W. Kinzelbach, Modeling of groundwater withdrawal and its consequences to the aquifer — A case study in semi-arid Botswana, report, Inst. of Hydromech. and Water Resour. Manage., Swiss Federal Inst. of Technol. Zurich, Zurich, Switzerland, 1997.

Simmers, I., Estimation of natural groundwater recharge, in *Proceedings of NATO Advanced Research. Workshop, Antalya, Turkey, March 1987*, *NATO ASI Ser., Ser. C*, vol. 222, edited by I. Simmers, D. Reidel, Norwell, Mass., 1988.

Sitar, N., J. D. Cawlfield, and A. Der Kiureghian, A first-order reliability approach to stochastic analysis of subsurface flow and solute transport, *Water Resour. Res.*, *23*(5), 794–804, 1987.

Skaggs, T. H., and D. A. Barry, The first-over reliability method of predicting cumulative mass flux in heterogeneous porous formations, *Water Resour. Res.*, *33*(6), 1485–1494, 1997.

Smith, L., and R. A. Freeze, Stochastic analysis of steady state groundwater flow in a bounded domain, 2, Two-dimensional simulations, *Water Resour. Res.*, *15*(6), 1543–1559, 1979.

Tang, D. H., and G. F. Pinder, Simulation of groundwater flow and mass transport under uncertainty, *Adv. Water Resour.*, *1*(1), 25–30, 1977.

Tiedemann, C., and S. M. Gorelick, Analysis of uncertainty in optimal groundwater contaminant capture design, *Water Resour. Res.*, *29*(7), 2139–2153, 1993.

Townley, L., Numerical models of groundwater flow: Prediction and para-

meter estimation in the presence of uncertainty, Ph.D. thesis, Dep. of Civ. Eng., Mass. Inst. of Technol., Cambridge, 1983.

Townley, L. R., and J. L. Wilson, Computationally efficient algorithms for parameter estimation and uncertainty propagation in numerical models of groundwater flow, *Water Resour. Res.*, *21*(12), 1851–1860, 1985.

Wellfield Consulting Services, Main report, Palla Road groundwater resources investigation, Phase 1, report, Gaborone, Botswana, 1994.

Wood, W., and W. E. Sanford, Chemical and isotopic methods for quantifying ground-water recharge in a regional, semiarid environment, *Groundwater*, *33*(3), 458–468, 1995.

Xiang, Y., and S. Mishra, Probabilistic multiphase flow modeling using the limit-state method, *Groundwater*, *35*(5), 820–824, 1997.

Yeh, W. W.-G., Review of parameter identification procedures in groundwater hydrology: The inverse problem, *Water Resour. Res.*, *22*(2), 95–108, 1986.

Zoellmann, K., and W. Kinzelbach, Use of a numerical flow and transport model in the interpretation of environmental tracer data, paper presented at ModelCARE 96, Colo. Sch. of Mines, Golden, 1996.

W. Kinzelbach and T. Siegfried, Institute for Hydromechanics and Water Resources Management, Swiss Federal Institute of Technology Zürich, ETH Hönggerberg, CH-8093 Zürich, Switzerland. (Kinzelbach@ihw.baug.ethz.ch; Siegfried@ihw.baug.ethz.ch)

H. Kunstmann, Institute for Meteorology and Climate Research-Atmospheric Environmental Research, Karlsruhe Research Center Technology and Environment, Kreuzeckbahnstrasse 19, D-82467 Garmisch-Partenkirchen, Germany. (harald.kunstmann@imk.fzk.de)